J|A|C|S COMMUNICATIONS

Published on Web 09/10/2009

Hyperthermal O-Atom Exchange Reaction $O_2 + CO_2$ through a CO_4 Intermediate

Laurence Y. Yeung,[†] Mitchio Okumura,*[,†] Jeffrey T. Paci,[‡] George C. Schatz,*[,§] Jianming Zhang,[||] and Timothy K. Minton*[,||]

Division of Chemistry and Chemical Engineering, California Institute of Technology, Pasadena, California 91125, Department of Chemistry, University of Victoria, Victoria, British Columbia V8W 3V6, Department of Chemistry, Northwestern University, Evanston, Illinois 60208-3113, and Department of Chemistry and Biochemistry, Montana State University, Bozeman, Montana 59717

Received May 14, 2009; E-mail: mo@caltech.edu; schatz@chem.northwestern.edu; tminton@montana.edu

O_2 and CO_2 do not react under ordinary conditions. This can be attributed to the large activation energy for multiple double-bond cleavage, as Dixon illustrated in his early experiments in which dry $CO-O_2-CO_2$ mixtures "did not explode" when subjected to a spark discharge.[1] Otomo et al.[2] later reported a reaction of CO_2 and electronically excited O_2* when they observed O_3 products after irradiating super- and subcritical O_2/CO_2 mixtures with UV light. While investigating the isotope exchange reaction

$$^{16}O(^3P) + {}^{12}C^{18}O_2 \rightarrow {}^{18}O + {}^{16}O^{12}C^{18}O \qquad (1)$$

at hyperthermal collision energies in a crossed-molecular-beam experiment, we found evidence for the gas-phase oxygen isotope exchange reaction

$$^{16}O_2 + {}^{12}C^{18}O_2 \rightarrow {}^{18}O^{16}O + {}^{16}O^{12}C^{18}O \qquad (2)$$

of ground-state reactants at high collision energies (~160 kcal mol^{-1}). Our observations on the dynamics of this reaction, taken together with the results of ab initio calculations of stationary points on the lowest triplet potential energy surface (PES), suggest a plausible adiabatic mechanism for the reaction of O_2 with CO_2 through a CO_4 transition complex.

Crossed-molecular-beam experiments were performed with a hyperthermal oxygen source containing ~89% $O(^3P)$ and ~11% $O_2(^3\Sigma_g^-)$.[3] A pulsed beam of $^{16}O(^3P)$ and $^{16}O_2$ (at an unknown vibrational temperature) was velocity-selected with a chopper wheel at an average velocity $\langle v \rangle = 8262$ m s^{-1} [see the Supporting Information (SI)]. The resulting beam was crossed at a right angle with a pulsed, supersonic beam of 98% $^{12}C^{18}O_2$ gas (2% $^{16}O^{12}C^{18}O$). $^{12}C^{18}O_2$ and $^{16}O^{12}C^{18}O$ products were detected at *m/z* 48 ($^{12}C^{18}O_2^+$) and 46 ($^{16}O^{12}C^{18}O^+$) with a rotatable mass spectrometer that collected number density distributions as a function of arrival time, $N(t)$, at a given laboratory angle, Θ (the angle at which the $^{16}O^{12}C^{18}O$ scatters with respect to the direction of the reagent oxygen beam). Time-of-flight (TOF) distributions for $^{16}O(^3P)$, $^{16}O_2$, $^{12}C^{18}O_2$, and $^{16}O^{12}C^{18}O$ were collected over a range of laboratory angles (6−54°); at each angle, the TOF distribution was integrated to give a laboratory angular distribution $N(\Theta)$. A forward-convolution method was used to derive the center-of-mass (c.m.) translational energy and angular distributions $P(E_T)$ and $T(\theta_{c.m.})$, respectively, from the laboratory $N(t)$ and $N(\Theta)$ distributions,[4] where $\theta_{c.m.}$ is the angle at which $^{16}O^{12}C^{18}O$ scatters with respect to the reagent oxygen direction in the c.m. frame.

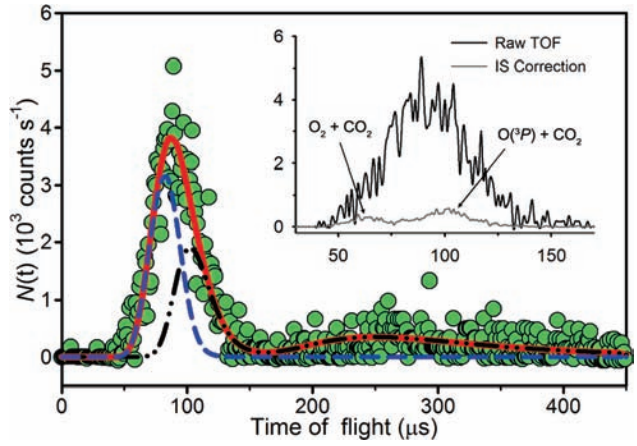

Figure 1. Laboratory TOF distribution for *m/z* 46 ($^{16}O^{12}C^{18}O^+$; green circles) at $\Theta = 6°$ with the inelastic scattering signal removed, shown with the $O(^3P) + CO_2$ (dot-dashed black line), $O_2 + CO_2$ (dashed blue line), and summed (solid red line) forward-convolution fits. Flight times less than 72 μs violate energy conservation for $^{16}O(^3P) + {}^{12}C^{18}O_2$. The inset compares the raw TOF distribution with the IS TOF distribution, which is subtracted.

The inset in Figure 1 shows a raw *m/z* 46 TOF distribution of $^{16}O^{12}C^{18}O$ products recorded at $\Theta = 6°$. A small fraction of the signal that is attributable to inelastic scattering (IS) of $^{16}O^{12}C^{18}O$ impurities in the CO_2 beam by ^{16}O and $^{16}O_2$ can be subtracted. The remaining signal, shown in Figure 1, represents $^{16}O^{12}C^{18}O$ products from O-atom exchange reactions of $^{12}C^{18}O_2$.

We initially expected the reactive *m/z* 46 signal to arise from reactions of $^{12}C^{18}O_2$ with the ^{16}O atoms (reaction 1) with a broad distribution of c.m. collision energies (E_{coll}) peaked at 98.8 kcal mol^{-1} and having a full width at half-maximum (fwhm) of 18 kcal mol^{-1}. However, at small laboratory angles, we observed products with velocities that would violate energy conservation for this $O(^3P) + CO_2$ reaction (e.g., $t < 72$ μs in Figure 1). There is some uncertainty in the E_{coll} distribution because the exact time- and point-of-origin of the hyperthermal oxygen is not well-defined in the source, a free-jet expansion of a laser-induced plasma. This results in some uncertainty in the product flight times, which we estimate to be ±2 μs. Another small flight-time uncertainty arises in the forward-convolution fits because of uncertainty in the $^{12}C^{18}O_2$ beam velocity (see the SI). Still, we observed $^{16}O^{12}C^{18}O$ products arrive 10−20 μs faster than the minimum times allowed by the distribution of available energies, E_{avail} (≈E_{coll}; the zero-point-energy change is +0.1 kcal mol^{-1}), for reaction 1. Previous experience with this source indicates that neither ions nor electronically excited O atoms are present in the beam.[5]

We therefore hypothesize that the fast $^{16}O^{12}C^{18}O$ products come from reaction of $^{12}C^{18}O_2$ with $^{16}O_2$ in the hyperthermal beam. Because the velocity-selected $^{16}O_2$ molecules have the same laboratory-frame

[†] California Institute of Technology.
[‡] University of Victoria.
[§] Northwestern University.
[||] Montana State University.

10.1021/ja903944k CCC: $40.75

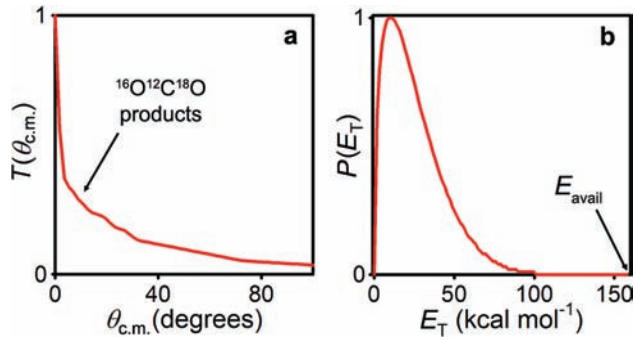

Figure 2. Center-of-mass-frame (a) angular and (b) translational energy distributions from the $^{16}O_2 + {}^{12}C^{18}O_2$ oxygen isotope exchange reaction obtained from TOF fits of *m*/*z* 46. The peak of the distribution of available energies is $E_{avail} = 158$ kcal mol^{-1}. Only the experimentally accessible range of c.m. angles ($\theta_{c.m.} < 100°$) is shown.

velocity distribution as the ^{16}O atoms, the $^{16}O_2$ molecules collide with the $^{12}C^{18}O_2$ molecules at substantially higher c.m. energies (peaked at $E_{coll} = 158$ kcal mol^{-1} with fwhm = 28 kcal mol^{-1}). Thus, $^{16}O^{12}C^{18}O$ products from reaction 2 have sufficient E_{avail} to account for the fastest products detected. The *m*/*z* 46 signal would then contain products of both reactions 1 and 2, the fastest products arising exclusively from reaction 2.

$P(E_T)$ and $T(\theta_{c.m.})$ distributions for reactions 1 and 2 were simultaneously obtained from forward-convolution fits of the *m*/*z* 46 TOF distributions. The results for the $^{16}O_2 + {}^{12}C^{18}O_2$ reaction are presented in Figure 2; $^{16}O(^3P) + {}^{12}C^{18}O_2$ results will be presented elsewhere. The presence of signal at flight times violating energy conservation for $^{16}O(^3P) - {}^{12}C^{18}O_2$ collisions was used to guide the fitting process, because the TOF distributions do not resolve the products unambiguously. Thus, we cannot rule out an additional dynamical channel in reaction 1 contributing to some of the signal we attribute to reaction 2, because energy conservation in reaction 1 is only violated at small lab angles.

The $^{16}O^{12}C^{18}O$ products scattered mainly in the forward direction ($\theta_{c.m.} = 0°$), though there was significant sideways scattering. Experimental sensitivity in the backward direction was insufficient to detect backward-scattered $^{16}O^{12}C^{18}O$ products, so forward−backward symmetric scattering (i.e., evidence for a long-lived intermediate complex) could not be ruled out. At these collision energies, however, an intermediate is unlikely to survive for a rotational period. The average total translational energy distribution for the two products was 25 kcal mol^{-1}, or 16% of the available energy; the $P(E_T)$ distribution was peaked at $E_T = 10$ kcal mol^{-1}. We estimate the yield for reaction 2 to be ≤2% of all O_2-CO_2 collisions. This estimate is an upper limit, because the complete Newton circle for inelastically scattered $^{16}O_2 + {}^{12}C^{18}O_2$ products was not observed in these experiments. Vibrational excitation of the O_2 may also be important in promoting the reaction, but the vibrational temperature of O_2 present in the expanded plasma is unknown.

Our experimental results are consistent with a $^{16}O^{12}C^{18}O$ product that rebounds from the $^{12}C^{18}O_2$ reactant's initial direction after it collides with O_2; this mechanism is characteristic of reactions with substantial activation energies that require high collision energies. The highly peaked angular distribution is consistent with a direct mechanism or a very short-lived intermediate. More surprising is the substantial internal energy of the products, which is much greater than that found for similar oxygen isotope exchange reactions for $O(^3P) + CO$, $O(^1D) + CO_2$, and $O + O_2$.[3,6,7] This large translational-to-internal energy conversion suggests that the reaction proceeds through an intermediate species that facilitates efficient translational-to-internal energy transfer or by a nonadiabatic transition to another electronic surface.

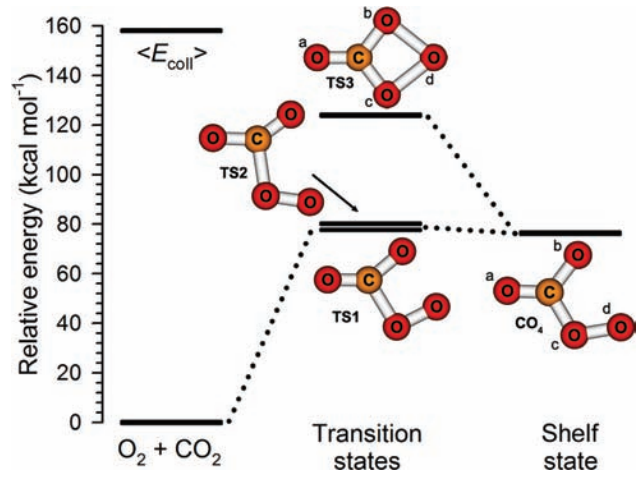

Figure 3. Calculated energies and structures on the lowest triplet PES of $O_2 + CO_2$. TS3 connects isoenergetic isomers of the CO_4 shelf (see SI).

On average, 134 kcal mol^{-1} of internal energy is available to the two products. This excess energy could be distributed among the five vibrational and four rotational degrees of freedom in O_2 and CO_2. Alternatively, this energy could be in the form of electronically excited products, including the $a^1\Delta_g$, $b^1\Sigma_g^+$, and $A^3\Sigma_u^+$ states of O_2 and the a^3A'' state of CO_2, which lies 119 kcal mol^{-1} above $CO_2(^1\Sigma_g^+)$.[8] The mass-spectrometric detection, however, does not allow us to determine the electronic states of the products.

Other reaction channels are possible. We cannot rule out a $CO_2 + O + O$ product channel because we did not collect sufficient data on the counterfragment $^{18}O^{16}O$. However, the energetically allowed $CO_2 + O(^3P) + O(^3P)$ channel ($\Delta H = 118$ kcal mol^{-1}) is spin-forbidden, and spin conservation would instead favor $O(^1D) + O(^3P)$ products, for which the energetic threshold of 163 kcal mol^{-1} is above the average E_{avail} in the experiment. There is also sufficient energy to form $O_3 + CO$ or $O + CO_3$[9] and to dissociate CO_2 to form $O_2 + O + CO$, but because we were not anticipating these reactions, we did not search for the relevant detectable products.

To investigate whether an adiabatic mechanism exists for the O_2-CO_2 isotope exchange reaction, we performed ab initio calculations to find stationary points on the lowest triplet PES for the $O_2 + CO_2$ reaction at the CCSD(T)/aug-cc-pVTZ level of theory. We identified two transition states (TS1 and TS2) connecting $O_2 + CO_2$ reactants with a triplet shelf state [$CO_4(^3A'')$; see Figure 3]. All three structures are planar. One atom of the oxygen molecule approaches the carbon atom of CO_2 and surmounts an activation barrier of 77.9 kcal mol^{-1} over TS1 to form a weak C−O bond and a $CO_4(^3A'')$ shelf (76.4 kcal mol^{-1}, just 1.5 kcal mol^{-1} below TS1) similar to a weakly bound CO_4 complex found at the B3LYP level of theory.[10,11] At 121.8 kcal mol^{-1}, we identified an effective transition state for $CO_4(^3A'')$ isomerization, TS3 (see the SI), containing a four-membered ring involving the carbon atom and three oxygen atoms. It resembles the bound $CO_4(^1A_1)$ structure lying 52.5 kcal mol^{-1} below it, although with a longer O_c-O_d bond; both structures have C_{2v} symmetry.[10−12]

Thus, a possible pathway for oxygen isotope exchange occurs through the forward and reverse directions of the following three steps: $O_2 + CO_2 \rightarrow [CO_4]^‡$ (TS1/TS2) $\rightarrow CO_4(^3A'') \rightarrow [CO_4]^‡$ (TS3). Spin-density maps depicting the singly occupied molecular orbitals (SOMOs) for CO_4 and TS3 (Figure 4) are consistent with this mechanism. $CO_4(^3A'')$ is a diradical with unpaired electron density concentrated in p-type orbitals of the single-bonded oxygens, O_b and O_d. This spin density is consistent with the radical character expected for an association of the O_2 diradical with the carbon atom of CO_2, because the unpaired electrons in O_2 are in orthogonal π_g*

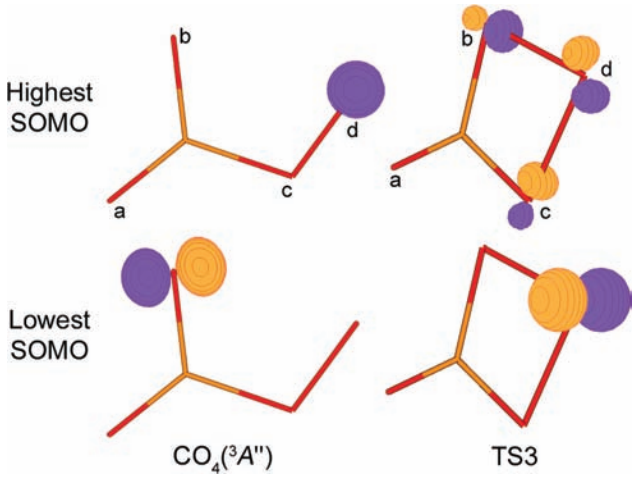

Figure 4. Singly occupied molecular orbitals (SOMOs) in the $CO_4(^3A'')$ and TS3 structures. Surfaces containing 70% of the electron density are shown. Notably, the highest SOMO of $CO_4(^3A'')$ and the lowest SOMO of TS3 have electron density primarily on O_d, suggesting that the SOMO is a spectator during isomerization.

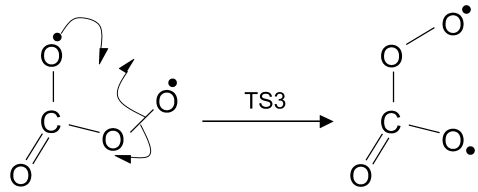

Figure 5. Electron-pushing diagram of an adiabatic $CO_4(^3A'')$ isomerization through TS3. See the SI for the complete proposed mechanism.

orbitals: as one C−O bond is formed between the in-plane π_g* antibonding orbital of O_2 and the in-plane π_u bonding orbital of CO_2 (the higher-energy π_g nonbonding orbital does not interact because of symmetry; see the SI), the out-of-plane π_g* orbital on O_2 is a relative spectator to the O_2 radical addition. This interaction, along with the bending of the CO_2, produces the SOMOs for $CO_4(^3A'')$ shown in Figure 4. In TS3, the lowest SOMO contains localized electron density on O_d in an out-of-plane p-type orbital, suggesting that the unpaired electron on O_d continues to be a spectator during $CO_4(^3A'')$ isomerization. The highest SOMO, however, contains delocalized electron density, with antibonding (σ*) character, in the plane of the molecule. This σ* character may be interpreted as electron density taken from the lowest SOMO in $CO_4(^3A'')$ and localized onto O_c during isomerization.

These theoretical results imply that an adiabatic mechanism exists for the oxygen isotope exchange reaction between O_2 and CO_2. During the isomerization of $CO_4(^3A'')$, the O_c-O_d σ bond is cleaved homolytically (Figure 5): one electron moves to a p-type orbital on O_c, while the other electron forms a bond with the unpaired electron on O_b. This pathway can account for the σ* character of the highest-energy SOMO in TS3 (the O_b-O_d bond takes an electron from the O_c-O_d bond), and it preserves radical character on O_d. Thus, the $^3A''$ symmetry is preserved throughout the association, isomerization, and dissociation steps.

This mechanism is qualitatively consistent with the small reaction cross section and a preference for rebounding reactive collisions inferred from the dynamics observed in the experiment. The O_2 must approach the CO_2 at very low impact parameters with high energies in order to overcome the initial barrier (TS1/TS2) and reach the "shelf" of the bound $CO_4(^3A'')$. Momentum along the reaction coordinate beyond $CO_4(^3A'')$ with ~80 kcal mol^{-1} excess energy should further compress the $C-O_c$ bond with synchronous bending of the $C-O_c-O_d$ angle, stretching of O_c-O_d, and ring formation to form TS3, which is followed by rapid repulsion from the final TS1/TS2 state. Finally, the large change in geometry from reactants to TS3 should facilitate the transfer of some translational energy into internal degrees of freedom of the products. Reactive scattering should become less "rebound"-like (forward scattered) as E_{coll} is increased above the reactive threshold; at 37 kcal mol^{-1} above the reactive barrier, the tight transition state, repulsive exit channel leading out of TS1/TS2, and low angular momentum must limit the extent of sideways scattering. While some sideways scattering is indeed observed in the experiment, the E_{coll} dependence of $T(\theta_{c.m.})$ is not known.

A nonadiabatic transition to another potential surface cannot be excluded, especially given the high internal energies observed in the products. At these high collision energies [80 kcal mol^{-1} above even the $CO_4(^3A'')$ shelf state], many excited-state surfaces must exist, and radiationless transitions via conical intersections may occur. While intersystem crossing (ISC) in the exit or entrance channels is unlikely at the high relative velocities of the experiment,[13] spin transitions could readily occur if a complex is formed. For instance, the bridging oxygen atom in TS3, O_d, must be equivalently bound to O_b and O_c, and chemical intuition suggests that an intersection with a singlet surface may occur by spin-paired $CO_4(^1A_1)$.[10−12]

In summary, an O_2-CO_2 isotope exchange reaction on the ground triplet electronic surface is possible and is consistent with our laboratory observations. Nevertheless, additional work would be valuable. Collision-energy-dependence studies of the product angular distribution may elucidate the mechanistic origins of the low average translational energy of the products. Experimental detection of O_2 counterfragments and a search for products from other channels (e.g., spectroscopic identification of electronically excited states) would also be revealing. Lastly, a more complete surface, reactive trajectories, and locations of possible surface intersection seams leading to ISC are vital for a full explanation of the reaction dynamics.

Acknowledgment. We thank G. B. Ellison, S. L. Mielke, and J. E. Wulff for insightful discussions. This work was supported by the Missile Defense Agency under cooperative agreement HQ0006-05-2-0001. L.Y.Y. was supported by the Davidow Fund, and G.C.S. was supported by AFOSR Grant FA955D-07-1-0095.

Supporting Information Available: Newton diagrams and TOF distributions of $^{16}O^{12}C^{18}O$ products, results of theoretical calculations, allowed product channels, and the proposed mechanism. This material is available free of charge via the Internet at http://pubs.acs.org.

References

(1) Dixon, H. *J. Chem. Soc., Trans.* **1886**, *49*, 94.
(2) Otomo, J.; Oshima, Y.; Takami, A.; Koda, S. *J. Phys. Chem. A* **2000**, *104*, 3332.
(3) Brunsvold, A. L.; Upadhyaya, H. P.; Zhang, J.; Cooper, R.; Minton, T. K.; Braunstein, M.; Duff, J. W. *J. Phys. Chem. A* **2008**, *112*, 2192.
(4) Lee, Y. T. In *Atomic and Molecular Beam Methods*; Scoles, G., Ed.; Oxford University Press: New York, 1988; Vol. 1, p 533.
(5) Troya, D.; Schatz, G. C.; Garton, D. J.; Brunsvold, A. L.; Minton, T. K. *J. Chem. Phys.* **2004**, *120*, 731.
(6) Perri, M. J.; Van Wyngarden, A. L.; Lin, J. J.; Lee, Y. T.; Boering, K. A. *J. Phys. Chem. A* **2004**, *108*, 7995.
(7) Van Wyngarden, A. L.; Mar, K. A.; Boering, K. A.; Lin, J. J.; Lee, Y. T.; Lin, S.-Y.; Guo, H.; Lendvay, G. *J. Am. Chem. Soc.* **2007**, *129*, 2866.
(8) Braunstein, M.; Duff, J. W. *J. Chem. Phys.* **2000**, *112*, 2736.
(9) Mebel, A. M.; Hayashi, M.; Kislov, V. V.; Lin, S. H. *J. Phys. Chem. A* **2004**, *108*, 7983.
(10) Cacace, F.; de Petris, G.; Rosi, M.; Troiani, A. *Angew. Chem., Int. Ed.* **2003**, *42*, 2985.
(11) Elliott, B. M.; Boldyrev, A. I. *J. Phys. Chem. A* **2005**, *109*, 3722.
(12) Jamieson, C. S.; Mebel, A. M.; Kaiser, R. I. *Chem. Phys. Lett.* **2007**, *440*, 105.
(13) Landau, L. *Phys. Z. Sowjetunion* **1932**, *2*, 46.

JA903944K